Computational Mechanics 23 (1999) 420–429 © Springer-Verlag 1999

Green's function formulation of laplace's equation for electromagnetic crack detection

T. A. Cruse, A. P. Ewing, J. P. Wikswo

1 Introduction

The two-dimensional Green's function for crack problems in potential theory is developed for application to the steady-state electromagnetic problem in three dimensions. The Green's function formulation is for a single, straight crack contained within or intersecting a regular boundary. The Green's function formulation for potential theory is validated using boundary element modeling of the Mode III, pure (antiplane) shear fracture mechanics problem.

The Green's function formulation is then used to model the three- dimensional magnetic field for the steady-state current flow through a two-dimensional plate with a plane crack. The BIE formulation is used to compute the normal component of the magnetic field for an arbitrary remote sensing location. This component of the magnetic field can be detected by a superconducting quantum interference device (SQUID) which is under research development for detecting cracks in aerostructures.

The required boundary integrals involve the tangential current flow on all boundaries including that for the crack. The explicit form for each of the two crack tip singularity terms is derived. The problem is validated with experimental data taken by a research SQUID system for a plate containing a single, thin slot representing the crack.

The use of special Green's functions for two dimensional cracks in elasticity is well established. The first application for straight cracks in anisotropic elastic plates was given by Snyder and Cruse (1975). The Green's function was derived at the same time for micromechanics applications by Sinclair and Hirth (1975). The use of the Green's function to obtain crack tip stress intensity factor path integrals was demonstrated by Snyder and Cruse (1975) and by Stern et al. (1976); a later application of this path integral was given by Kim (1985).

Applications of the Green's function method have been made to curved cracks, branched cracks, and multiple cracks, as in Rudolphi and Koo (1985) and Ang (1986). A Green's function for a crack interacting with an inclusion has also been developed by Li and Chudnovsky (1994). A summary of these and other BIE fracture mechanics advances is given in Cruse (1996).

T.A. Cruse✉, A.P. Ewing, J.P. Wikswo
Vanderbilt University, School of Engineering,
5332 Stevenson Center, Nashville, Tennessee 37232, USA

Correspondence to: T.A. Cruse

The authors gratefully acknowledge the support of the Air Force Office of Scientific Research, University Research Initiative, AFOSR Grant F49620-93-0268, under the direction of Dr. A. Weinstock. One of us, A. P. Ewing, gratefully acknowledges financial support of the Air Force AASSERT grant F49620-94-1-0369.

2 The two dimensional electromagnetic potential theory problem

The target problem is the prediction of the gradient of the three dimensional magnetic field created by steady current flow through a two dimensional plate containing one or two cracks coming from a hole. The electrical field problem in two dimensions is solved using the Green's function formulation for the two-dimensional crack problem.

We then apply three-dimensional potential theory to get the induced magnetic field normal to the plate. All three-dimensional aspects of the current flow problem in the finite thickness plate are ignored and the two-dimensional current flow is integrated over the finite thickness of the plate to get the three-dimensional magnetic vector at a specified field location. The normal component of the magnetic field is detected at that location using a fine-scale magnetometer type of device.

The following few equations summarize the problem of the electromagnetic (EM) field problem for steady current flow through a body with a crack. The surfaces are be assumed to be perfectly insulating except for the surfaces of current injection and removal. The conservation of charge is a side condition for this Neumann problem. The following derivations are based on the equations and definitions in Lorrain 1988.

The vector electrical field for the steady-state electrical conduction problem $\vec{E}(q)$ is taken to be the negative gradient of a harmonic function.[1]

$$\vec{E}(q) = -\vec{\nabla} V(q) \tag{1}$$

The current vector $\vec{J}(q)$ is scaled from the electrical field by the conductivity σ which is taken to be a constant for the body.

$$\vec{J}(q) = \sigma \vec{E}(q) \tag{2}$$

The steady current flow problem means that the electrostatic potential $V(q)$ is harmonic, $\nabla^2 V = 0$.

[1] The upper case letters (P, Q) are used to denote boundary points, while the lower case letters (p, q) are used to denote domain points.

The boundary conditions for the conductor are given in terms of the current flow density across the boundary defined by its outward normal $\hat{n}$ unit vector.

$$\vec{J}(Q)\cdot\hat{n}(Q) = -\sigma\frac{\partial V}{\partial n} = \sigma g(Q) \tag{3}$$

For insulated portions of the boundary, $g(Q) = 0$. Thus, we have a Neumann problem to solve with the BIE, for the potential V. The boundary integral equation (BIE) for this problem is summarized below.

$$\int_S [V(Q) - V(P)]\frac{\partial \Psi(P,Q;a)}{\partial n(Q)}\,\mathrm{d}S(Q) = \int_S \Psi(P,Q;a)g(Q)\,\mathrm{d}S(Q) \tag{4}$$

The physical interpretation of the requirement for the solvability of this Fredholm equation of the First Kind is that the total current flow is conserved. When we account for the fact that parts of the regular boundary are also insulated, we get the final form of the EM-BIE for our application.

$$\int_S [V(Q) - V(P)]\frac{\partial \Psi(P,Q;a)}{\partial n(Q)}\,\mathrm{d}S(Q) = \int_{S_N} \Psi(P,Q;a)g(Q)\,\mathrm{d}S(Q) \tag{5}$$

The solution of the EM-BIE is by the use of boundary element modeling of the surface and the imposition of boundary data interpolatives for each boundary element. The EM-BIE code is based on the algorithm in Cruse (1978) except that we now use quadratic variations for all boundary data, straight-line boundary elements, and exact integration of the boundary element terms.

3
Complex variable, two-dimensional BIE formulation

The required field problem is that of Laplace's equation subject to mixed boundary conditions which may locally be Dirichlet or Neumann conditions. We will formulate a two-dimensional boundary integral equation (BIE) for this problem using a special fundamental solution that corresponds to a surface upon which the normal derivative of the solution is zero. All other surfaces will have user-specified values of the potential or its normal derivative.

The field equations are for the unknown potential $\phi(p)$ where $p(\mathbf{x})$ is the two-dimensional Cartesian field point. The BIE will be formulated from a Green's identity using the fundamental solution of Laplace's equation and is denoted $\psi(p,q)$ where p, q are the field point and the singular point, respectively.

The fundamental solution in two dimensions is given by real part of the complex logarithm function. Recall that a real part of a complex function is one-half of the function plus its complex conjugate. We can then write the logarithmic potential as the following real form.

$$\psi(p,q) = [\log(z-c) + \log(\bar{z}-\bar{c})]/2 = \mathscr{R}\log(z-c) \tag{6}$$

where $c = x_p + iy_p$, $z = x_q + iy_q$ and $i = \sqrt{-1}$.

The required Green's function for the stated problem is the sum of the logarithmic fundamental solution and a function that will cancel the values of the normal derivative of the logarithm term at the crack surface. That is, the normal derivative of the sum of the two potentials is to be zero at the crack surface.

The required boundary values for our problem are taken to be the same on both the upper and lower side of the crack Γ. The straight crack will be taken for convenience to be along the real axis, centered at the origin, with the length $2a$. We denote the real location along the crack with the parameter $-a \le t \le a$. The boundary conditions are then given parametrically for the upper and lower crack surfaces as follows:

$$h^+(t) = \beta(t)$$
$$h^-(t) = \beta(t) \tag{7}$$

We denote the parametric location of the crack the following combinations of these boundary conditions hold for the Hilbert problem we have defined, e.g. England (1971). The general solution allows the potential to be discontinuous at the surface Γ.

$$h^+(t) - h^-(t) = 0$$
$$h^+(t) + h^-(t) = 2\beta(t) \tag{8}$$

The solution for this Hilbert problem is given by Snyder and Cruse (1975).

$$h(z) = \frac{1}{\pi\sqrt{z^2-a^2}}\int_\Gamma \frac{\beta(t)\sqrt{a^2-t^2}\,\mathrm{d}t}{t-z} + \frac{P(z)}{\sqrt{z^2-a^2}} \tag{9}$$

In this equation, the integral is performed on the positive side of the crack, from the left hand end $t = -a$ to the right hand end $t = +a$. The function of integration is a positive power polynomial which can be determined by the behavior of $h(z)$ at infinity. In what follows, we will compute only the real part of this integral.

We now take the boundary values $\beta(t)$ to be such that they cancel the boundary conditions of the normal (y) derivatives of the logarithmic fundamental solution. The superposition of two functions gives us a new fundamental solution whose y-derivative is zero on the crack surfaces. Recalling the fundamental solution to be given by the following expression

$$\psi(z,c) = \mathscr{R}[\log(z-c)] = \frac{1}{2}[\log(z-c) + \log(\bar{z}-\bar{c})] \tag{10}$$

we can derive the y-derivative of the logarithmic potential at the crack, which is parallel to the x-axis. We will take the negative of the derivative as our boundary conditions for the Hilbert problem. The final solution we seek will have zero y-derivative at the crack by adding the Hilbert problem potential to the fundamental solution potential.

$$\left.\frac{\partial\psi(z,c)}{\partial y}\right|_{z=x} = \frac{1}{2}\left[\frac{i}{x-c} - \frac{i}{x-\bar{c}}\right] = -\beta(x) \tag{11}$$

It is seen that the boundary condition is a real function on the crack surface Γ.

The Green's function is a real function with the boundary conditions satisfying the values $\beta(x)$; we will take this real function to be given by $G(p, q; a)$. The Hilbert problem potential is then given by the following integral.

$$G(p,q;a) = -\frac{1}{2\pi}\mathscr{R}\left[\frac{1}{\sqrt{z^2-a^2}}\int_\Gamma \frac{\sqrt{a^2-t^2}}{t-z}\left(\frac{i}{t-c}-\frac{i}{t-\bar{c}}\right)\mathrm{d}t\right] \tag{12}$$

The above integrals for the Green's function terms exist in closed form, as can be seen in England (1971). We need only the real part for each of the above terms, as in Snyder and Cruse (1975), given as follows

$$G(p,q;a) = \mathscr{R}[h(z)] = -\frac{1}{2}\mathscr{R}\left[\frac{i}{\sqrt{z^2-a^2}}\left(\frac{I(z)-I(c)}{z-c}-\frac{I(z)-I(\bar{c})}{z-\bar{c}}\right)\right] \tag{13}$$

where the integral $I(z)$ is defined below

$$I(z) = \frac{1}{\pi}\int_{-a}^{+a}\frac{\sqrt{a^2-t^2}}{t-z}\,\mathrm{d}t = \left[\sqrt{z^2-a^2}-z\right] \tag{14}$$

for all z except along the crack where $I(z)$ has the boundary values

$$I^+(t) = \left[i\sqrt{t^2-a^2}-t\right]$$
$$I^-(t) = \left[-i\sqrt{t^2-a^2}-t\right] \quad t \in \Gamma \tag{15}$$

The complex potential $h(z, c)$ has been used to find a Hilbert problem solution for the boundary data derived from the y-derivatives of the fundamental solution. These terms will be used for the evaluation of the BIE terms involving the y-derivative.

The BIE also requires that we have the fundamental solution potential, and not just its y-derivative. Therefore, we have to integrate the function $h(z)$ with respect to z/i to have the function whose boundary conditions on the crack we have just used. The integration result is given as follows (see Cruse 1978).

$$\mathscr{G}(p,q;a) = \mathscr{R}\left[\frac{1}{i}\int h(z,c)\,\mathrm{d}z\right] = -\frac{1}{2}\mathscr{R}[J(z,c;a)-J(z,\bar{c};a)] \tag{16}$$

where $J(z, c)$ is given by the following result

$$J(z,c;a) = \log\left[2\frac{\sqrt{z^2-a^2}\sqrt{c^2-a^2}+cz-a^2}{\left(z+\sqrt{z^2-a^2}\right)\left(c+\sqrt{c^2-a^2}\right)}\right] \tag{17}$$

such that

$$\frac{\partial J}{\partial z} = \frac{I(z)-I(c)}{(z-c)\sqrt{z^2-a^2}} \tag{18}$$

We now have the two Hilbert problem forms that are needed to modify the BIE for the crack problem. The new potential $J(z, c; a)$ depends on both field points as well as the crack size. The crack for this formulation is limited to a straight crack along the real axis with its center at the origin. For computational purposes, we use a simple shift and rotation of the coordinate axes to put the crack at any user-defined location and orientation relative to the physical geometry.

The final BIE formulation for the crack problem is obtained by taking the sum of the original fundamental solution with the solution of the Hilbert problem. This modified fundamental solution which satisfies the insulated condition on the crack surface is denoted a Green's function for the crack. That is, the Green's function is an harmonic function containing the fundamental singularity property and it satisfies the boundary conditions on the crack. This fundamental solution is denoted by $\Psi(p, q)$ and is given by the real part (denoted by the $\mathscr{R}$ notation) of the two terms. The original fundamental solution term has been normalized by dividing it by 2π.

$$\Psi(p,q;a) = \frac{1}{2\pi}\left[\mathscr{R}\log(z-c)-\frac{1}{2}\mathscr{R}\{J(z,c;a)-J(z,\bar{c};a)\}\right] = \frac{1}{4\pi}\mathscr{R}[\log(z-c)+\log(\bar{z}-\bar{c}) - J(z,c;a)+J(z,\bar{c};a)] \tag{19}$$

The modified fundamental solution, or Green's function, for the crack is shown containing the crack length as a parameter. This is to reinforce that the presence of the crack is now embedded in the fundamental solution terms. The Green's function derivative in the normal direction at the surface point Q will also be needed for the BIE formulation. That result is now given.

$$\frac{\partial\Psi(p,Q;a)}{\partial n} = \frac{1}{4\pi}\mathscr{R}\left[\frac{n_x+in_y}{z-c}+\frac{n_x-in_y}{\bar{z}-\bar{c}}-\frac{(n_x+in_y)}{\sqrt{z^2-a^2}} \times\left(\frac{I(z)-I(c)}{z-c}-\frac{I(z)-I(\bar{c})}{z-\bar{c}}\right)\right] = \frac{1}{2\pi}\mathscr{R}\left[\frac{n_x+in_y}{z-c}\right]-\frac{1}{4\pi}\mathscr{R}\left[\frac{(n_x+in_y)}{\sqrt{z^2-a^2}} \times\left(\frac{I(z)-I(c)}{z-c}-\frac{I(z)-I(\bar{c})}{z-\bar{c}}\right)\right] \tag{20}$$

The BIE identity can now be written on the total of the regular surface and the crack surface.

$$0 = \int_S[\phi(Q)-\phi(P)]\frac{\partial\Psi(P,Q;a)}{\partial n(Q)} - \int_S\Psi(P,Q;a)\frac{\partial\phi(Q)}{\partial n(Q)}\,\mathrm{d}S(Q) + \int_\Gamma[\phi(Q)-\phi(P)]\frac{\partial\Psi(P,Q;a)}{\partial n(Q)} - \int_\Gamma\Psi(P,Q;a)\frac{\partial\phi(Q)}{\partial n(Q)}\,\mathrm{d}S(Q) \tag{21}$$

The effect of the special Green's function formulation is now seen. Both integrals on the crack surface Γ are zero. The first is zero due to the Green's function having zero

normal derivative on the crack, and the second due to the insulating boundary conditions for the unknown potential function.

Thus, we take as the final BIE for the insulated crack potential theory problem to be the following equation.

$$0 = \int_S [\phi(Q) - \phi(P)] \frac{\partial \Psi(P, Q; a)}{\partial n(Q)} - \int_S \Psi(P, Q; a) \frac{\partial \phi(Q)}{\partial n(Q)} \, dS(Q) \tag{22}$$

The BIE models the crack through the Green's function, and not through the boundary of the crack. The form that has been derived places the crack at the origin and oriented along the x-axis. However, the existing computer program allows the user to specify the global location of the crack and its orientation. The crack can be contained within the region or can intersect one or more physical surfaces. Again, the BIE code has been written to accept these cases.

Thus, the BIE for the insulated crack problem contains only the uncracked surface in the BIE. Application of the special Green's function to the elasticity problem has demonstrated the very high accuracy of this formulation for crack problems, as in Cruse (1978). Further, applications of the special Green's function formulation have demonstrated a high degree of accuracy for cracks at holes and other stress concentrating geometries, see Cruse (1988).

4
Interior derivatives of the potential

The interior potential for the Green's function formulation is given by the identity

$$\phi(p) = \int_S \phi(Q) \frac{\partial \Psi(p, Q; a)}{\partial n(Q)} - \int_S \Psi(p, Q; a) \frac{\partial \phi}{\partial n}\bigg|_Q \, dS(Q) \tag{23}$$

The derivatives in the x-direction and the y-direction of the interior potential are needed for the full electromagnetic field formulation.

$$\frac{\partial \phi(p)}{\partial(x_c, y_c)} = \int_S \phi(Q) \frac{\partial^2 \Psi(p, Q; a)}{\partial n(Q) \partial(x_c, y_c)} - \int_S \frac{\partial \Psi(p, Q; a)}{\partial(x_c, y_c)} \frac{\partial \phi}{\partial n}\bigg|_Q \, dS(Q) \tag{24}$$

The derivative at the point c of the kernels given in Eqs. (19) and (20) are required in order to compute the gradient of the interior potential. These kernel derivatives are given as follows.

$$\frac{\partial \Psi(p, Q; a)}{\partial(x_c, y_c)} = -\frac{1}{2\pi} \mathscr{R}\left[\frac{(1, i)}{z - c}\right] - \frac{1}{4\pi} \mathscr{R}\left[\frac{(1, i)}{\sqrt{c^2 - a^2}} \left(\frac{I(z) - I(c)}{z - c}\right) - \frac{(1, -i)}{\sqrt{\bar{c}^2 - a^2}} \left(\frac{I(z) - I(\bar{c})}{z - \bar{c}}\right)\right] \tag{25}$$

The identity

$$\frac{\partial J}{\partial c} = \frac{I(c) - I(z)}{(c - z)\sqrt{c^2 - a^2}} = \frac{I(z) - I(c)}{(z - c)\sqrt{c^2 - a^2}} \tag{26}$$

has been applied using the symmetry of $J(z, c; a)$ with respect to z, c.

The derivative at c of the normal derivative kernel function in Eq. (20) is given in the following set of terms.

$$\frac{\partial^2 \Psi(p, Q; a)}{\partial n \partial(x_c, y_c)} = +\frac{1}{2\pi} \mathscr{R}\left[\frac{(n_x + i n_y)(1, i)}{(z - c)^2}\right] - \frac{1}{4\pi} \mathscr{R}\left[\frac{(n_x + i n_y)(1, i)}{\sqrt{z^2 - a^2}} \left(\frac{\partial}{\partial c} \frac{I(z) - I(c)}{z - c}\right)\right] + \frac{1}{4\pi} \mathscr{R}\left[\frac{(n_x + i n_y)(1, -i)}{\sqrt{z^2 - a^2}} \left(\frac{\partial}{\partial \bar{c}} \frac{I(z) - I(\bar{c})}{z - \bar{c}}\right)\right] \tag{27}$$

The remaining derivatives with respect to z above are given in the following result.

$$\frac{\partial}{\partial c} \frac{I(z) - I(c)}{z - c} = \frac{I(c)}{(z - c)\sqrt{c^2 - a^2}} + \frac{I(z)}{(z - c)^2} \tag{28}$$

5
Crack tip field intensity factors

One of the key parameters in crack problems is the so-called crack tip intensity factor (CIF = K) derived from the derivatives of the potential at each crack tip. The CIF is given by the following limit

$$K_{(x,y)} = \lim_{c \to \pm a} \sqrt{2\pi(c \mp a)} \frac{\partial \phi(z, c; a)}{\partial(x, y)} \tag{29}$$

for $z \neq c$. The intensity factor can be derived for any direction of approach to either of the crack tips. For convenience, we will take the point $c = \pm(a + r)$ where the real variable r is the distance from the crack tips and is taken to be along the x-axis. Thus, $\bar{c} = c$ for the limiting processes. The CIF is then given by the following integral identity.

$$K_{(x,y)}|_{\pm a} = \lim_{r \to 0} \sqrt{2\pi r} \frac{\partial \phi(p)}{\partial(x, y)} = \lim_{r \to 0} \sqrt{2\pi r} \int_S \left(\phi(Q) \frac{\partial^2 \Psi(p, Q)}{\partial(x, y) \partial n(Q)} - \frac{\partial \Psi(p, Q)}{\partial(x, y)} \frac{\partial \phi(Q)}{\partial n(Q)}\right) dS \tag{30}$$

Carrying out the limits on the two kernel functions, one finds that the derivative $\partial\phi/\partial x$ is zero ahead of the crack. That is, the gradient of the flux parallel to the crack is zero for potential theory. The singular term is contained solely in $\partial\phi/\partial y$, the gradient transverse to the crack, ahead of the crack. One can also find from a study of the kernels that the gradients for points on the crack surfaces are swapped and the sign changed. Thus, for the top crack surface $\partial\phi/\partial x$ is singular with the CIF equal to minus that of the approach ahead of the crack, output in the code as K. The derivative $\partial\phi/\partial y$ is, by the Green's function, zero along the crack surfaces.

The two kernels that are needed in order to compute K for the limit using points ahead of the crack are given as follows, using the right hand crack tip $c = +a$. The code allows the negative crack tip computation as well.

$$\lim_{r\to 0}\sqrt{2\pi r}\frac{\partial^2\Psi(p,Q)}{\partial y\partial n(Q)} = \sqrt{\frac{a}{4\pi}}\mathscr{R}\left[\frac{i(n_x+in_y)}{(z-a)\sqrt{z^2-a^2}}\right] \quad (31)$$

$$\lim_{r\to 0}\sqrt{2\pi r}\frac{\partial\Psi(p,Q)}{\partial y} = -\frac{1}{\sqrt{4\pi a}}\mathscr{R}\left[\frac{i[I(z)-I(a)]}{z-a}\right] \quad (32)$$

The boundary element method (BEM) replaces the actual boundary with an approximate boundary discretized as a finite set of simple elements. The current algorithm uses straight line segments in order that we can implement analytical integrations of the kernels in Eqs. (19) and (20). The boundary functions are then represented by quadratic interpolations over each boundary segment. Continuity of the potential is enforced, but not continuity of the flux, between the boundary elements. The analytical integrations of the two kernels times quadratic polynomial interpolations of the boundary data are computed on an element-by-element basis. The details of the boundary element analytical integrations are contained in the dissertation by Ewing (1998).

5.1
Test problem for antiplane shear loaded crack

The test problem is the antiplane-shear fracture mechanics problem governed by Laplace's equation $\nabla^2 w(x,y)$ for the equilibrium equation in terms of the displacement function $w(x,y)$. The two shear stresses (denoted by τ_{xz} and τ_{yz} where z is normal to the plane) correspond to the gradients of the potential in the x, y directions. Thus, the formulated Green's function corresponds to the exact solution for a large plate containing a central crack remotely loaded by the applied shear traction $\partial\phi/\partial n$. Equilibrium of the boundary tractions is given by the side-condition

$$\oint_S \frac{\partial w(x,y)}{\partial n}\,\mathrm{d}S \equiv 0 \quad (33)$$

which must be satisfied for the solution to the BIE to exist.

The test problem is a large square plate containing a central crack of length $2a$ to simulate an infinite plate. The crack is taken to have various angles β relative to the global x-axis for the test problems. The test problems are loaded by constant antiplane-shear values of τ_{yz} on the upper and lower surfaces.

The validation criteria for the numerical solutions are the shear stress intensity factor, referred to as the Mode III stress intensity factor in fracture analysis. The intensity factor for the infinite plate loaded by a constant $\tau_{yz} = \tau_0$ at infinity is given by the following result from Sneddon and Lowengrub (1969).

$$K_{III} = \tau_0\sqrt{\pi a} \quad (34)$$

In the case of the angled crack the solution is found in the handbook by Tada et al. (1985) to be given as follows:

$$K_{III} = \tau_0\cos\beta\sqrt{\pi a} \quad (35)$$

The exact displacement field solution for points on the crack surfaces (corresponding to the values of the potential in the field) is given by Sneddon and Lowengrub (1969) as follows:

$$\frac{w(x\in\Gamma,0)}{a} = \frac{\tau_0}{\mu}\sqrt{1-\left(\frac{x}{a}\right)^2} \quad (36)$$

The singular stress terms near the crack tip are given as follows:

$$\tau_{xz} = -\frac{K_{III}}{\sqrt{2\pi r}}\sin\frac{\theta}{2}$$
$$\tau_{yz} = +\frac{K_{III}}{\sqrt{2\pi r}}\cos\frac{\theta}{2} \quad (37)$$

The numerical results of the EM-BEM confirm the validity of the formulation. The EM-BEM code reproduces the exact solution for the stress intensity factor, the shear stress gradient along the crack, and the displacements along the crack. The accuracy relative to the above analytical solutions for the infinite body is 0.004 , and can be further improved by increasing $W/2a$, which was taken to be 100 for the test problems. The EM-BEM code is therefore taken to be validated.

6
The three-dimensional magnetic field problem

The vector magnetic field $\vec{B}$ at an arbitrary point in space but caused by the steady current is derived according to the law of Biot-Savart according to Lorrain et al. (1988). We will take the three dimensional field point for the determination of the magnetic field as the point $s(\mathbf{x})$. In general, this point will be taken at some distance z from the mid-plane of the two-dimensional plate with a central crack.

The magnetic field is given as the curl of the current field divided by the distance between the coil point and the integration point. The result, written for the *three dimensional problem*, is given as follows.

$$\vec{B}(s) = \frac{\mu_0}{4\pi}\int_R \vec{\nabla}_s\times\left(\frac{\vec{J}(q)}{r(s,q)}\right)\mathrm{d}V(q) \quad (38)$$

where μ_0 is the free space permeability constant. Note that the gradient is taken at the free-space point s and not the integration point q. The gradient could be taken outside of the integral and lead to a different potential formulation for the non-steady state solution. We will leave the gradient inside the integration for our developments.

The result can also be written in terms of the electrical current potential $V(q)$, which substitution is valid for the steady-state electromagnetic formulation, as given in Eq. (1).

$$\vec{B}(s) = -\frac{\mu_0\sigma}{4\pi}\int_R \vec{\nabla}_s\times\left(\frac{\vec{\nabla}_q V(q)}{r(s,q)}\right)\mathrm{d}V(q) \quad (39)$$

At this time we can expand the gradient operator as follows

$$\vec{\nabla}_s \times \left(\frac{\vec{\nabla}_q V(q)}{r(s,q)} \right) = - \vec{\nabla}_q \times \left(\frac{\vec{\nabla}_q V(q)}{r(s,q)} \right) + \frac{\vec{\nabla}_q \times \vec{\nabla}_q V(q)}{r(s,q)} \tag{40}$$

However, the last term above is zero due to taking the curl of a gradient of a scalar field. We can then write the following form in terms of the derivatives at q.

$$\vec{\nabla}_s \times \left(\frac{\vec{\nabla}_q V(q)}{r(s,q)} \right) = - \vec{\nabla}_q \times \left(\frac{\vec{\nabla}_q V(q)}{r(s,q)} \right) \tag{41}$$

The derivatives are now all at the point q and we can drop the notation of the derivative point. We now use Stokes' theorem to convert the volume integral into the equivalent surface integral, as follows. The form of Stoke's theorem for the current application is now given,

$$\int_V \vec{\nabla} \times \vec{F} \, \mathrm{d}V = \oint \hat{n} \times \vec{F} \, \mathrm{d}S \tag{42}$$

where $\hat{n}$ is the surface normal. The model problem is a plate with contours defined in the x-y plane and two parallel surfaces offset from each other in the z-direction. Thus, if we take the z-component of the left-hand side of Eq. (42), the resulting surface integrals are on the two-dimensional contours for the plate being analyzed. It is this component of the gravity field that we wish to model. The second identity converts the cross-product term to the following dot-product term.

$$\begin{aligned} \hat{e}_3 \cdot (\hat{n} \times \vec{F}) &= (\hat{e}_3 \times \hat{n}) \cdot \vec{F} \\ &= \hat{t} \cdot \vec{F} \end{aligned} \tag{43}$$

and thus

$$\int_V \hat{e}_3 \cdot (\vec{\nabla} \times \vec{F}) \, \mathrm{d}V = \oint \hat{t} \cdot \vec{F} \, \mathrm{d}S \tag{44}$$

Substituting the results from Eqs. (39) and (40) into Eq. (44), we obtain the necessary boundary integrals for the B_3 component of the magnetic field in terms of the current flow along the boundaries of the two-dimensional plate.

$$B_3(s) = B_z(s) = \frac{\mu_0 \sigma}{4\pi} \int_{S+\Gamma} \frac{\vec{\nabla} V(Q) \cdot \hat{t}}{r(s,Q)} \, \mathrm{d}S(Q) \tag{45}$$

The modeling approach that is to be used for the EM-applications is to be quasi-three dimensional. We take the current to be defined for two dimensional slices parallel to the surface of the plate. Each slice has a two dimensional surface and crack geometry, although the crack geometry can be changed for each layer to simulate a three dimensional crack. The quasi-three dimensional approach neglects flow components in the direction normal to the surface of the plate. This approximation may be valid if changes in the geometry in the direction normal to the plane of the plate are small.

The tangent vector in the above magnetic field problem is now unique and is the vector tangent to the two dimensional surface which has been employed in the EM-BIE formulation. The tangential derivatives of the potential V at the boundary can therefore be determined from the EM-BIE solution, including points on the crack tip. Analytical derivation of the special Green's function to get the tangential derivatives is used to compute the singular current flow at the crack tip. However, the above form is still in three dimensional form and its integration will be discussed in the next section.

$$\vec{\nabla}_p V(p) \cdot \vec{t} = -\frac{1}{2\pi} \int_S [V(Q) - V(P)] \frac{\partial^2 \Psi(p,Q;a)}{\partial n \partial t} \, \mathrm{d}S(Q) + \frac{1}{2\pi} \int_S \frac{\partial V(Q)}{\partial n} \frac{\partial \Psi(p,Q;a)}{\partial t} \, \mathrm{d}S(Q) \tag{46}$$

The magnetic field at $s(\mathbf{x})$ is derived from a volume potential converted to the surface tangential current flow problem. If the current flow was truly two dimensional, the two dimensional result for the magnetic field would convert the above equation to the $\log(z-c)$ form used for the fundamental solution. Clearly, the quasi-three dimensional approach contains the most critical three dimensional elements of the magnetic field problem and can probably serve well in the current application, is spite of the current flow approximations used.

The integral from Eq. 45 is written again in the local coordinate system of the measurement device, as follows

$$B_z(s) = -\frac{\mu_0 \sigma h}{4\pi} \int_{S+\Gamma} \frac{\vec{\nabla} V(Q) \cdot \hat{t}}{r(s,Q)} \, \mathrm{d}S(Q) \tag{47}$$

where h is the thickness of the plate. The EM-BEM algorithm calculates $\mathrm{d}V/\mathrm{d}t$ as a piecewise linear result since we are taking $V(Q)$ to be represented as piecewise quadratic. This integration is done for all boundary elements except for the crack surface Γ. Substituting this V_t into the integral for $B_z(s)$ gives the contribution to the magnetic field at point s due to all boundaries except for the crack surface, Γ.

The BIE for the electromagnetic problem is written in two-dimensions. The magnetic field created by the current flow around the crack in two dimensions is three-dimensional. The three-dimensional EM-BEM evaluations for the magnetic field for linear boundary elements in two-dimensions is illustrated in Fig. 1. The integrals are discussed in greater detail in Ewing (1998).

For points on the crack surface, the singular behavior of V_t at the crack tip requires special consideration. The complete analytic representation of V_t for crack problems

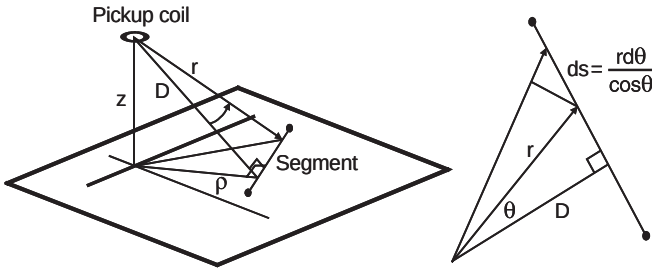

Fig. 1. Integration geometry between pickup coil and boundary segment

is given by Westergaard (1939) as equivalent to the following analytical form:

$$V_t = \frac{f_1(x)}{\sqrt{x^2 - a^2}} + f_2(x) \tag{48}$$

where $f_1(x)$ and $f_2(x)$ are analytic functions of the real position x on the crack and a is the crack half-length. The first term in Eq. (48) contains the discontinuity at the crack tip while the second term is needed to match far field (away from the crack) boundary conditions. On the crack surface, Eq. (48) can be rewritten as

$$\begin{aligned} V_t|_\Gamma &= \frac{if_1(x)}{\sqrt{a-x}\sqrt{a+x}} + f_2(x) \\ &= \frac{1}{\sqrt{R}} \frac{if_1(x)}{\sqrt{a+x}} + f_2(x) \\ &= \frac{1}{\sqrt{R}} iF_1(x) + f_2(x) \end{aligned} \tag{49}$$

where R is the distance measured from the crack tip at $x = a$. For the region near the positive crack tip, the behavior of V_t is known to follow

$$V_t = \frac{K^-}{\sqrt{2\pi R}} \sin\frac{\beta}{2} \tag{50}$$

where K^+ is the crack intensity factor (CIF) at the $x = +a$ crack tip. Note that at $R = 0$ (crack tip), $V_t = \infty$. If there are two crack tips in the modeled region, then there is a corresponding V_t term proportional to K^-.

Due to the singular behavior of V_t at the crack tip, numerical integration is necessary to evaluate the magnetic field contribution of the crack. Values of V_t are evaluated for the upper and lower crack surfaces using the BIE program and then the magnetic field is calculated through a numerical integration of the previously stated Biot-Savart relation (Eq. 47).

Numerical integration over the crack is accomplished using discretization of the crack boundary into elements. We use a coordinate transformation, V_t expressed in terms of nodal values and interpolation functions (or shape functions) of the intrinsic coordinate ξ, see Burnett (1987). Once mapped into ξ-space, Gaussian quadrature numerical integration is used to evaluate the integral. The present formulation uses quadratic interpolation functions $N_m(\xi)$ which require three nodes per boundary element.

Each half of the crack is modeled using one crack-tip element containing the crack-tip node and one regular element, each element being defined by three nodes (see Fig. 2). The regular element is a straight-forward use of the interpolation functions but the crack-tip element requires some modification to accommodate the singularity at the crack tip. The crack-tip element contains the crack tip node as its first node and the mapping uses the quarter-point formulation of Burnett (1987) to account for the inverse square-root singular behavior at the crack tip. The other regular element will use the general form of the shape functions to map them to ξ-space.

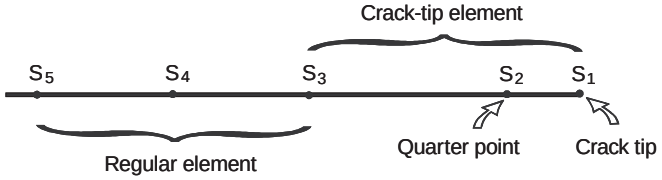

Fig. 2. Crack divided into regular and quarter point (crack-tip) elements

For the crack-tip element on the upper crack surface, the standard mapping to ξ-space needs to be modified to accommodate the $1/\sqrt{t}$ behavior of $V_t(t)$ at the crack tip. In what follows, the crack tip point will be mapped at $t = 0$. The general approach will be to split the $V_t(t)$ term into a singular term multiplied times a non-singular coefficient. The form of $V_t(t)$ follows from Eq. (49).

$$\begin{aligned} V_{\mathrm{t}}(t)|_\Gamma &= \frac{if(t)}{\sqrt{t}\sqrt{2L - t}} \\ &= \frac{1}{\sqrt{t}} F_1(t) \end{aligned} \tag{51}$$

To map $V_t(t)$ into ξ-space, the singular term will use an inverse mapping relation and the non-singular term will use the quadratic shape functions. To determine the inverse mapping relation, we start with the $1/\sqrt{t}$ behavior which can be represented by placing the mid node of the quadratic element at the quarter point location

$$t_2 = \frac{1}{4}(t_3 - t_1) \tag{52}$$

Therefore, choosing $t_1 = 0$, $t_2 = \frac{1}{4}L$, $t_3 = L$ as shown in Fig. 2, the quarter point mapping is given by the following result

$$t = (1 - \xi^2)\frac{L}{4} + \frac{1}{2}\xi(1 + \xi)L \tag{53}$$

which has a corresponding inverse mapping given as follows

$$\xi = -1 + 2\sqrt{\frac{t}{L}} \tag{54}$$

The Jacobian J is given by

$$\begin{aligned} J = \frac{\mathrm{d}t}{\mathrm{d}\xi} &= -2\xi\frac{L}{4} + \frac{1}{2}(1 + 2\xi)L \\ &= \frac{L}{2}(1 + \xi) \end{aligned} \tag{55}$$

Note that at the $t = 0$ ($\xi = -1$) point the Jacobian also equals zero. This characteristic is important when evaluating the integral of the mapped function. The $1/\sqrt{t}$ term is represented in ξ-space by solving for $1/\sqrt{t}$ in terms of ξ in Eq. (54)

$$\frac{1}{\sqrt{t}} = \frac{2}{\sqrt{L}(\xi + 1)} \tag{56}$$

Therefore, the B_z contribution due to the crack-tip element on the upper crack surface is as follows

$$
\begin{aligned}
B_z|_\Gamma &= -\frac{\mu_0 \sigma h}{4\pi} \int \frac{V_t(t)}{r(t)}\, \mathrm{d}s \\
&= -\frac{\mu_0 \sigma h}{4\pi} \int_0^L \frac{1}{\sqrt{t}} \left(\frac{F(t)}{r(t)}\right) \mathrm{d}s \qquad (57) \\
&= -\frac{\mu_0 \sigma h}{4\pi} \int_{-1}^{+1} \frac{2}{\sqrt{L}(\xi+1)} \left[N_1(\xi) \left(\frac{F(t)}{r(t)}\right)_{t_1} \right. \\
&\quad \left. + N_2(\xi) \left(\frac{f(t)}{r(t)}\right)_{t_2} + N_3(\xi) \left(\frac{F(t)}{r(t)}\right)_{t_3} \right] \frac{L}{2} (\xi+1)\, \mathrm{d}\xi \\
&= -\frac{\mu_0 \sigma h}{4\pi} \sqrt{L} \int_{-1}^{+1} \left[N_1(\xi) \left(\frac{F(t_1)}{r(t_1)}\right) \right. \\
&\quad \left. + N_2(\xi) \left(\frac{F(t_2)}{r(t_2)}\right) + N_3(\xi) \left(\frac{F(t_3)}{r(t_3)}\right) \right] \mathrm{d}\xi
\end{aligned}
$$

Note that as $\xi \to -1$ the singular term ($\xi + 1$ in denominator) goes to infinity but is canceled by the Jacobian term ($\xi + 1$ in numerator) going to zero, thereby making the overall function well behaved in the mapped space. All values of F, r, and t are known except for F at the crack tip node which has the singularity. But at the crack tip, the value of the function is the CIF(K^+)

$$
F(t_1) = \frac{K^+}{\sqrt{2\pi}} \qquad (58)
$$

The same operation can be performed to get the value at the negative crack tip. All boundaries are now taken care of and the following section summarizes the experimental validation of the measurement model based on this development.

7
Experimental validation of the EM-BEM code

A measurement model has been developed using this BIE/EM formulation. The program simulates the scanning of a Superconducting Quantum Interference Device (SQUID) magnetometer, see Jenks et al. (1997), over a sample containing a crack. The SQUID magnetometer uses small pickup coils to sense magnetic field above the sample. Injecting a uniform DC-current in the sample causes the current to be parallel to the sample's surface under the pickup coil. The associated magnetic field is mostly tangential to the plate surface for scans located centrally and with small lift-off distances. A flaw in the specimen will perturb the current distribution and produce a vertical magnetic field component that can then be detected by the SQUID. When the SQUID is scanned two-dimensionally over the sample, a magnetic field map is produced, revealing a flaw signature that commonly has a dipolar shape (maximum and minimum peaks).

As a measurement reference, electrodischarge machined (EDM) slots and saw cuts are used in calibrating NDE systems for detection of cracks. A combination of a drilled hole with an EDM slot is an approximation to a crack emanating from an aircraft fastener hole. Fabrication of test samples made this way is simple and controllable making it easy to build a test set representing the range of conditions that are of interest. But measurements with NDE instruments by Rummel et al. (1991) have shown that the instrument response is not necessarily the same as that from a fatigue crack of the same size and geometry. It is possible that crack closure may cause electrical conductivity across parts of the fatigue crack thus causing a reduced signal response over an electrically insulated slot. The EM-BEM code used for the SQUID measurement simulation is for a closed crack (no width) but electrically insulated along the entire length. Future work needs to address the slot versus crack issues.

The validation experiment used a 5 mA DC-current injected into a 75 mm × 150 mm × 0.03 mm copper clad circuit board containing a 15 mm × 0.03 mm slot cut with a scalpel (see Fig. 3). Although this setup does not provide completely uniform current injection across the sample (transverse to the slot) due to the point source electrodes, the region around the centrally located slot should be relatively uniform.

Figure 4 shows the contour map resulting from a 2D scan over the sample with the lines AA′, BB′, and CC′. Profiles along these lines on this map are compared to those calculated by the measurement model. The scaling factor between the measured signal response (a voltage) and the calculated magnetic flux was determined using these profiles. Magnetic field shape characteristics (matching of peaks and valleys) will reflect the accuracy of the measurement model since a difference between the model and experiment would show up as a mismatch of the profiles at either the edge or the crack locations.

The measurement model is in very good agreement with experiment for all profiles. A slight mismatch at the right side of AA′ can be seen and is most likely due to a small variation in the distance from the plate to the probe (liftoff) during a scan (i.e. that is the sample is not level).

8
Summary and conclusions

The problem formulation begins with a boundary-integral representation for Laplace's equation in the plane. The presence of a single, straight crack in the plane is represented by a special Green's function corresponding to zero flux across the crack. The Green's function used provides a very effective BIE model for the zero-flux boundary con-

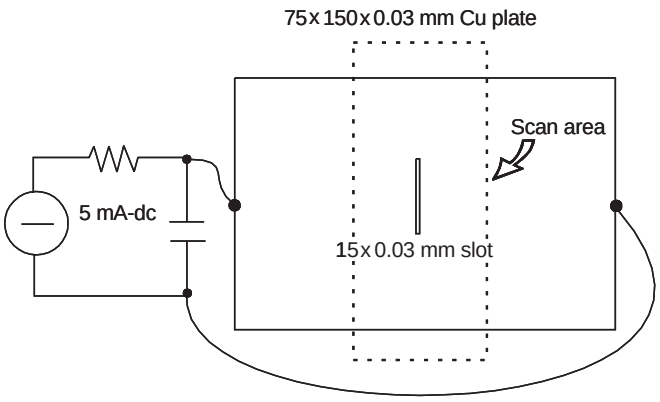

Fig. 3. Experimental setup for DC-current injection in copper plate with slot

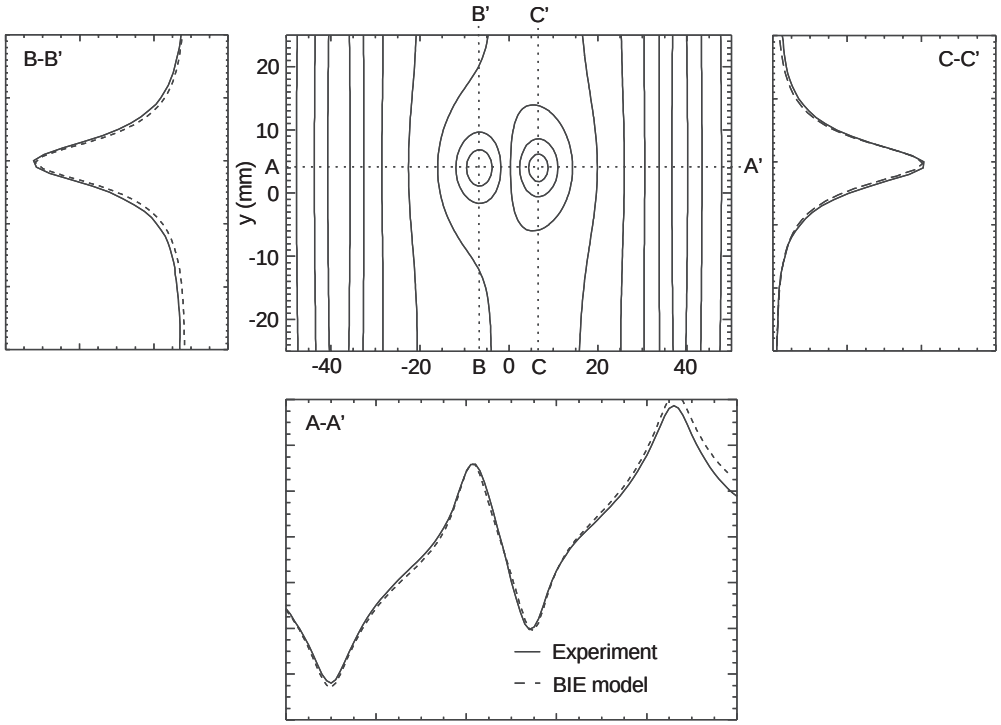

Fig. 4. Magnetic field contour map and profiles comparing experiment with the BEM model

dition as the crack then is a part of the integral equation kernels and is not a part of the modeled boundary. A boundary element implementation for the harmonic BIE uses quadratic data variation on piecewise linear boundary elements. The BEM model with the Green's function is validated for the antiplane shear crack problem for which exact solutions exist.

The steady-state electromagnetic problem suitable for calculating the magnetic field for a cracked plate with current injection has been formulated in terms of the derived BIE. The gradient of the potential yields the electrical field vector. The electromagnetic field equations yield the magnetic field at arbitrary three-dimensional space points, using the law of Biot-Savart. The law of Biot-Savart result is given in terms of two boundary integrals of current flow tangent to the boundaries which must be evaluated for all boundary points, including the crack. The cracked plate is represented as a finite thickness plate with a two-dimensional field so that the EM-BEM code results can be used in the three-dimensional magnetic field computation.

The magnetic field integrals on the boundary points are formulated as Gaussian quadratures for the quadratic EM-BEM data. The crack surface requires a special integration algorithm due to the singular conditions at each crack tip. Isoparametric boundary element algorithms are used for the magnetic field boundary integrals. The crack tip element uses the quarter-point mapping developed for BEM traction models of fracture problems which contain the leading term in the singular behavior. The mapping is shown to contain the leading term exactly.

The application problem is the magnetic field for the steady-state current flow through two-dimensional plate with a crack. The magnetic field is the normal component of the field, which is the component detected by an experimental SQUID magnetometer. Experimental data was obtained for a copper plate with an EDM slot representing a crack. The new BEM results for the magnetic field are used to simulate a SQUID scan over the plate along three scan lines parallel and normal to the current flow field. The agreement between the BEM results and the experimental data is excellent.

References

Ang WT (1986) A boundary integral solution for the problem of multiple interacting cracks in elastic media. Int. J. Fract. 31:259–270

Burnett DS (1987) Finite Element Analysis – From Concepts to Applications, Addison-Wesley Publishing Co., New York:305–327

Cruse TA (1988) Boundary Element Analysis in Computational Fracture Mechanics, Kluwer Academic Publishers, Dordrecht, The Netherlands

Cruse TA (1978) Two-dimensional BIE fracture mechanics analysis, Applied Mathematical Modeling, 2:287–293

Cruse TA (1987) Fracture Mechanics, Chapter 7, Boundary Element Methods in Mechanics, ed. D. E. Beskos, North-Holland, Amsterdam:333–365

Cruse TA (1996) BIE fracture mechanics analysis: 25 years of developments. Comput. Mech. 18:1–11

England AH (1971) Complex Variable Methods in Elasticity, Wiley-Interscience, London

Ewing AP (1998) SQUID NDE and POD Using a BEM Measurement Model, Ph.D. Dissertation, Vanderbilt University, Nashville, TN

Jenks WG, Sadeghi SSH, Wikswo Jr. JP (1997) SQUIDs for Nondestructive Evaluation, Journal of Physics D. Applied Physics 30:293–323

Kim J-W (1985) A contour integral computation of stress intensity factors in the cracked orthotropic plates. Eng. Fract. Mech. 21:353–364

Li R, Chudnovsky A (1994) The stress intensity factor Green's function for a crack interacting with a circular inclusion. Int. J. Fract. 67:169–177

Lorrain P, Corson DP, Lorrain F (1988) Electromagnetic Fields and Waves, W. H. Freeman and Company, New York
Rudolphi TJ, Koo LS (1985) Boundary element solutions of multiple, interacting crack problems in plane elastic media. Engineering Analysis, 2:211–216
Rummel WD, Moulder JC, Nakagawa N (1991) The Comparative Responses of Cracks and Slots in Eddy Current Measurements, Review of Progress in Quantitative NDE, 10, D. O. Thompson and D. E. Chimenti, Eds., Plenum, New York:277–283
Sneddon IN, Lowengrub M (1969) Crack Problems in the Classical Theory of Elasticity, John Wiley & Sons, Inc., New York: 37–39
Snyder MD, Cruse TA (1975) Boundary-integral equation analysis of cracked anisotropic plates. Int. J. Fract. 11(2):315–328
Stern M, Becker EB, Dunham RS (1976) A contour integral computation of mixed mode stress intensity factors. Int. J. Fract. 12:359–368
Tada H, Paris PC, Irwin G (1985) The Stress Analysis of Cracks Handbook, Section 5.2, Paris Productions Inc., St. Louis
Westergaard HM (1939) Bearing pressures and cracks. J. Appl. Mech. 61:A49–A53